Received: 1 Jun 2022 | Accepted: 4 Oct 2022 | Available online: 26 Oct 2022
DOI: http://dx.doi.org/10.18180/tecciencia.2022.33.5

TECCIENCIA

UNIVERSIDAD · ECCI

RESEARCH ARTICLE
Engineering

Finite Element Analysis of Composite Pressure Vessel Using Reduced Models

Análisis de Elementos Finitos para Recipientes a Presión Compuestos Mediante Modelos Reducidos

Junaid Jadoon [1] | **Atif Shazad** [2] | **Muhammad Muzamil** [2] | **Maaz Akhtar** [3] | **Mohsin Sattar** [4]

[1]Department of Mechanical Engineering, Pakistan Institute of Engineering & Applied Sciences Islamabad, Pakistan.

[2]Department of Mechanical Engineering, NED University of Engineering and Technology, Karachi, Pakistan

[3]Mechanical Engineering Department, Imam Muhammad Ibn Saud Islmmic University, Riyadh,11432 Saudi Arabia

[4] Department of Mechanical Engineering, Universiti Teknologi PETRONAS, Perak, Malaysia

Correspondence
Junaid Jadoon
Email: atifshahzad2717@gmail.com

Abstract. Pressure vessels are one of the essential industrial tools for high-pressure containments. Catastrophic failure of pressure vessels is detrimental to society. It is essential to design pressure vessels by selecting high-strength materials and analyzing them beyond working loads to ensure safety. Liner less composite cylinders have gained importance in the pressure vessel industry owing to their high strength-to-weight ratios, corrosion resistance, etc. However accurate and efficient prediction of their mechanical properties was required. Finite element methods were employed for the structural analysis of reduced models. The three-dimensional shell structure of the Graphite/Epoxy composite system was analyzed using APDL. Appropriate boundary conditions were applied to 5x reduced models internally pressurized to 20 MPa. Suitable mesh size was selected through mesh independence and stress distributions were discussed for reduced models, especially for the inner two layers. Comparison with previous research confirmed the validity of models. 0.1^{o} rotated strip of vessel gives accurate and conservative results. Tsai Wu, Tsai Hill, Maximum Shear Stress (Smax), and Von Mises were used to assess the failure of composite cylinders. Each of the failure criterion predicts the failure of the second layer for all the reduced models.

Keywords: Pressure vessel, Finite element methods, Graphite/Epoxy composite, Reduced models.

How to cite: Junaid Jadoon et al., **Finite Element Analysis of Composite Pressure Vessel Using Reduced Models**, TECCIENCIA, Vol. 17, No. 33, 49-62, 2022
DOI:http://dx.doi.org/10.18180/tecciencia.2022.33.5

Resumen

Los recipientes a presión son una de las herramientas industriales esenciales para las contenciones de alta presión. La falla catastrófica de los recipientes a presión resulta perjudicial para la sociedad. En este sentido es esencial diseñar recipientes a presión seleccionando materiales de alta resistencia y analizándolos más allá

de las cargas de trabajo para garantizar la seguridad. Los cilindros compuestos sin revestimiento han ganado importancia en la industria de recipientes a presión debido a su alta relación resistencia-peso, resistencia a la corrosión, etc. Sin embargo, se requería una predicción precisa y eficiente de sus propiedades mecánicas. Se emplearon métodos de elementos finitos (FEM por su siglas en inglés) para el análisis estructural de modelos reducidos. La estructura tridimensional de la cubierta del sistema compuesto de grafito/epoxi se analizó mediante APDL. Se aplicaron condiciones de contorno apropiadas a modelos reducidos $5\times$ presurizados internamente a 20 MPa. Se seleccionó el tamaño de malla adecuado a través de la independencia de la malla y se discutieron las distribuciones de tensión para modelos reducidos, especialmente para las dos capas internas. La comparación con investigaciones anteriores confirmó la validez de los modelos. La tira de vaso girada 0.1^o proporciona resultados precisos y conservadores. Tsai Wu, Tsai Hill, Maximum Shear Stress (Smax) y Von Mises se utilizaron para evaluar la falla de los cilindros compuestos. Cada uno de los criterios de falla predice la falla de la segunda capa para todos los modelos reducidos.

Palabras clave: recipiente a presión, métodos de elementos finitos, compuesto de grafito/epoxi, modelos reducidos

1 | INTRODUCTION

Advancement in the material field is keyway to gaining desired developments for a technically sound society. The appropriate material is highly recommended for any sort of load-bearing equipment and pressure-bearing structures. Pressure vessels are utilized around the entire globe for different applications like the strong acceptance of CNG in the transport sector. Due to the devastating effects of bursting, it is essential to sort out the maximum operational limit of stresses and allowable deformation due to internal pressure. Composite materials for pressure vessels are not very common but many industries are now shifting towards composite due to high anisotropic strength, low weight, and better corrosion resistance. Limiting the extreme values, research has been conducted on different composite materials to specify the failure amount by using finite element modeling software (FEA) [1].

A study was conducted by E.S.Barboza et al [2] to evaluate bursting pressure for the liner of the pressure vessel. Performance of liner of LLDPE & HDPE composite material shown that longitudinal fracture (brittle) at the center and transverse fracture (ductile) at the left end. The ideal thickness that can sustain bursting pressure of 20 bar was around 15mm. J.P. Xu et al [3] investigated the failures due to burst pressure and reduction in fatigue life of pressure vessels. This study focused on the unit load method for testing purposes and ABAQUS was used for predicting fatigue and structural strength. A Gaurav Singh et al [4] conducted study on Kevlar as base material and HDPE as a liner in the pressure vessel. Multi-layers of Kevlar and single-layer liner were investigated by Ansys 15 software. Results revealed that larger deformation was produced in a 25°degree orientation layer and minimum deformation resulted in a 35°degree orientation layer.

Takalkar et al [5] investigated the impact of winding angle on the composite overwrapped vessel. Structural analysis was performed by considering three shell model. The analysis was performed on T300/epoxy composite material. The appropriate winding angle was ± 35°, minimum stress and deflection resulted at this angle. It was shown that an increase in winding angle ultimately reduces stresses, however, the deflection remains constant till ± 35° but get increased beyond ± 35°. K. Jae-sung et al [6] researched variation in winding angle vide longitudinal and thickness direction. The winding angle difference between the first and last plies was calculated at around 18°. FEA techniques were utilized to investigate the possible results due to variation in winding orientations and compared with the experimental results. V.V Vasiliev et al [7] investigated the reinforcement of fibers in two directions by the persistent winding of fiber tapes in composite material shell structures and utilized them for commercial purposes in place of using unidirectional fiber for minimum mass in isotensiod vessels. M.Z. Kabir [8] studied the effect of the geodesic dome profile on the stress distributions over the pressure vessel. Dependent on stress conditions, a study revealed different shapes for mandrels and performed optimization in shapes.

Research conducted by M. Dimitrijevic et al [9] on ceramic matrix composite revealed the pros of indulging ceramics as fiber to obtain properties like high strength, high stiffness, high-temperature applications, enhanced fatigue life, high compressive strength, and applications under extreme environments and conditions. Metal matrix is utilized to augment ductility as well as electrical properties in the composite. Valuable properties were achieved due to this combination and the same were used in analysis and applications. X. L. Zhong Yuea et al [10] investigated the behavior of liner material like stresses and deformations under the applied pressures, design and burst pressures, and safe working environment of the pressure vessel. Cracks and crazes are the main failures in cylinder liners and were analyzed by using ANSYS. The study revealed that insufficient strength of liner material and inappropriate structure of cylinder were the major sources of defects.

T.H.L. Meng-Kao Yeh et al [11] researched composite pressure vessels to investigate their behavior with cross-ply symmetrical laminates at [0/90] degrees. Modifications in stacking sequence and composite material were evaluated to find appropriate criteria for failure. Results of the full pressure vessels model revealed that the graphite/epoxy structure failure, using the Tsai Hill failure criteria, occurred in the second layer and the first layer can withstand the stresses generated at the 30° axisymmetric fiber/epoxy model. Dhanireddy et al [12] adapted the model which is free from bending extension coupling allowing the use of transversally isotropic assumption within the FEA model. They performed the stress analysis of composite pressure vessels for an axisymmetric model.

Yongzheng Shao et al [13] conducted research on pressure cylinders, carbon/vinyl ester composite material was selected and different winding laminations were performed. The study revealed that carbon/vinyl ester showed good results concerning ultimate pressure as compared to simple epoxy as the matrix. Digital imaging techniques and strain/deformations were performed to check crack propagation under bursting pressure.

The impact of transverse loading repetition was investigated by Ibrahim Demir et al [14], and the results revealed that repetition of transverse loading generated considerable effects on the bursting pressure of composite pressure vessels. Glass/epoxy composite material was chosen, and multiple fiber orientations were selected to check the best result. A similar approach was performed on a vessel filled with water at a temperature around 70°C, the result showed a decrease in burst pressure. A study of using HDPE as liner and Glass fiber for winding was conducted by J.C. Velosa et al [15], Abaqus 6.5.1 FEM tool was used for analysis. Tsai Wu criteria indicated no failure upon 24 bar pressure for a 90° fiber orientation angle. Roham Rafiee et al [16] discussed failure under low-velocity impact and observed that higher impact energy produces major variation in delamination.

In the current study, a composite pressure vessel was analyzed using the Finite Element Methods tool named APDL, under different constraints and working conditions. Stress analysis and failure study were performed by using Tsai Wu, Tsai Hill, Maximum shear stresses (Smax), and Von Mises Stresses for the first two layers of the pressure vessel. The selection was based on the failure of the composite layers using the failure theories. Studies conducted recently were all related to full-scale models, this study focused on reduced models under the same working conditions. This study is performed to investigate the accuracy of reduced models in comparison with full-scale models

2 | THEORETICAL ANALYSIS

Pressure vessels are comprised of composite layers in hoop and helical directions. The classical Laminate theory is used to analyze the laminated composite structure. The considered composite structure was a thick one as the thickness to radius ratio was 0.2 [11]. For calculations, stress-strain tensors were used as follows,

$$\epsilon_i = S_{ij}\sigma_j$$

$$\sigma_i = C_{ij}\epsilon_j$$

where $C_ij = [S_{ij}]^{-1}$, ϵ_i , σ_i are strain and stress and C_{ij}, S_{ij} , being the stiffness and compliance matrices respectively. Further analyzing each ply of the transversally isotropic composite pressure vessel. The compliance matrix can be written as S_{ij} is defined as:

$$S_{ij} = \begin{bmatrix} \frac{1}{E_1} & -\frac{\nu_{12}}{E_2} & -\frac{\nu_{13}}{E_3} & 0 & 0 & 0 \\ -\frac{\nu_{12}}{E_2} & \frac{1}{E_1} & -\frac{\nu_{13}}{E_3} & 0 & 0 & 0 \\ -\frac{\nu_{12}}{E_2} & \frac{\nu_{13}}{E_3} & \frac{1}{E_3} & 0 & 0 & 0 \\ 0 & 0 & 0 & \frac{1}{G_{13}} & 0 & 0 \\ 0 & 0 & 0 & 0 & \frac{1}{G_{13}} & 0 \\ 0 & 0 & 0 & 0 & 0 & 2\left(\frac{1}{E_1} + \frac{\nu_{21}}{E_2}\right). \end{bmatrix}$$

This theory predicts the mechanical behavior of the angle ply anisotropic fiber-reinforced laminate.

2.1 | Failure theories

Tsai-Wu, Tsai Hill, and maximum stress failure criteria predict the failure of each layer of the laminate. Tsai Wu failure criteria [17] is defined as,

$$F_i\sigma_i + F_{ii}\sigma_i\sigma_j \geq 1$$

For transversally isotropic behavior, Tsai Wu criteria assume the following values of strength coefficients,

$$F_2 = F_3 = F_4 = F_5 = F_6 = 0, \quad F_{22} = F_{33}, \quad F_{55} = F_{66}, \quad \text{and} \quad F_{12} = F_{13}.$$

Tsai Wu failure criteria can be written as

$$F_1\sigma_1 + F_2(\sigma_2 + \sigma_2) + F_{11}\sigma_1^2 + F_{22}(\sigma_2^2 + \sigma_3^2) + 2F_{12}(\sigma_1\sigma_2 + \sigma_1\sigma_3) + 2F_{23}\sigma_2\sigma_3 + F_{44}\sigma_{23}^2 + F_{55}(\sigma_{12}^2 + \sigma_{13}^2) \geq 1$$

Where σ_i is stress and F_{ii} are the strength coefficients, E, G and ν are the elastic constants.

$$F_{11} = \frac{1}{X_tX_c}, \quad F_{22} = \frac{1}{Y_tY_c}, \quad F_{44} = \frac{1}{S_{23}^2}, \quad F_{55} = \frac{1}{S_{12}^2}$$

$$F_1 = \frac{1}{X_t} - \frac{1}{X_c}, \quad F_2 = \frac{1}{Y_t} - \frac{1}{Y_c}, \quad F_{12} = -\frac{1}{2}\sqrt{F_{11}F_{22}}$$

Tsai Hill failure criteria [11] predict similarly,

$$\frac{\sigma_1^2}{X^2} - \frac{\sigma_1\sigma_2}{X^2} - \frac{\sigma_2^2}{Y^2} - \frac{\tau_{12}^2}{S^2} = 1$$

Criteria of maximum stress delineate the failure of fibers [11],

$$\frac{\sigma_1}{X_t} \geq 1 \qquad \text{and} \qquad \frac{\sigma_1}{X_t} \geq 1$$

for compression

$$\frac{\sigma_1}{X_c} \geq 1 \qquad \text{and} \qquad \frac{\sigma_2}{Y_c} \geq 1$$

for shear $\tau_{12}/S \geq 1$ where X_t, X_c are the tensile and compressive strength in the fiber direction, Y_t, Y_c in the transverse direction, and S_{12}, S_{23} being the fiber and transverse direction shear strength.

The above equations tell us about the possible failure at some composite layer of the pressure vessel for the value greater than or equal to 1.

3 | RESEARCH METHODOLOGY

The research study was defined as a methodology that resulted in a better solution related to stress analysis, reduction in computing cost, computing time, and failure in composite layers. This study was focused on the comparison of reduced models of pressure vessels with full model pressure vessels. Reduced model accuracy was checked by calculating errors between Von mises stress values of reduced models and full model. The computational cost and time comparison between the full and reduced model was performed. After the selection of the geometry and loading conditions, it was necessary to define the materials to withstand applied loads along with the appropriate boundary conditions. After the selection of material was performed, a number of layers of the composite material were defined and the orientation of each layer was defined to conform to geometry. Shell type model was used in the ANSYS APDL. Meshing comprised of full, half, quarter, 90° rotated, 45° rotated, 1° rotated and 0.1° rotated mesh pressure vessel. The element type used was SHELL281. Models were varied with respect to the layer's orientation of material and analyzed for better results.

3.1 | Geometry Selection

CNG cylinder of dimensions shown in Table 1 were selected for analysis, opening diameter of 40 mm was used as input and output ports to the pressure vessel. All other physical dimensions for the high-pressure composite cylinder are represented in Table 1.

TABLE 1 Dimensions of Pressure Vessel.

Parameter	Dimensions (mm)
Overall length	808
Cylinder length	592.25
Opening diameter	40
Inner shell radius	89.75
Outside radius	107.75
Thickness	18
Dome Inner radius	89.75
Dome outer radius	107.75

3.2 | FEA Modeling

The FEA modeling was performed by Mechanical APDL which is a powerful tool for analysis of different working conditions under different constraints. FEA model of this pressure vessel comprised of defining the composite layers over the geometry drawn, then the boundary conditions and working environment were applied and meshing was done prior to the static structural solution of the model.

3.3 | Layer's Definition and Orientations:

Graphite/epoxy layers were defined over the shell structure. There was a total of 144 layers with cross-ply laminates that are symmetrical having an orientation of 0° to 90°. The thickness of the overall structure was 18 mm. Stacking of layer had performed in mechanical APDL and 06 layers stacking were very clear in Fig. 1

which indicate the orientation angle from 0 degrees to 90 degrees. The first layer's orientation was 0° and the second and third at 90° (from behind to the front), confirming the symmetrical cross-ply orientations of the composite layers. Similarly, all 144 layers are oriented.

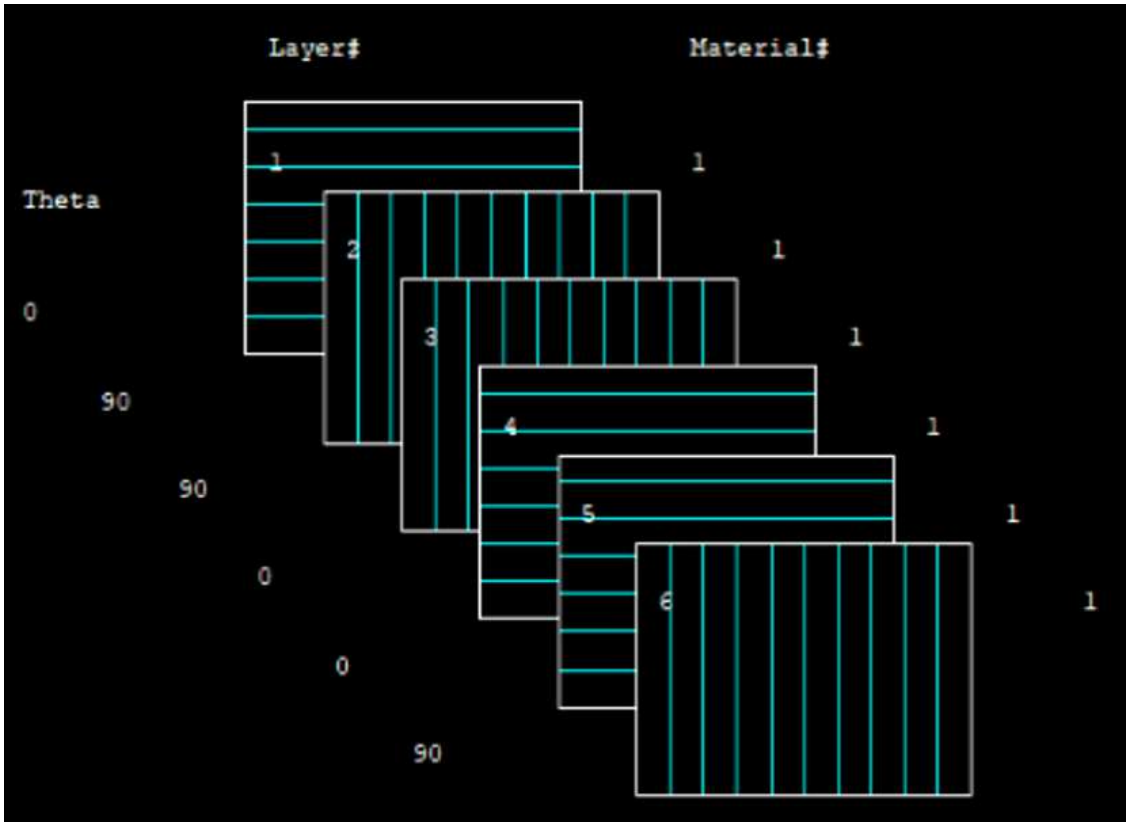

FIG. 1 Layers Orientations.

4 | LAYER'S DEFINITION AND ORIENTATIONS

Graphite/epoxy layers were defined over the shell structure. There was a total of 144 layers with cross-ply laminates that are symmetrical having an orientation of 0° to 90°. The thickness of the overall structure was 18 mm. Stacking of layer had performed in mechanical APDL and 06 layers stacking were very clear in Fig. 1 which indicate the orientation angle from 0 degrees to 90 degrees. The first layer's orientation was 0° and the second and third at 90° (from behind to the front), confirming the symmetrical cross-ply orientations of the composite layers. Similarly, all 144 layers are oriented.

4.1 | Boundary Conditions and Loading applications

Static pressure of 20 MPa was applied to all the models under consideration. Fig. 2 includes all reduced models and full model constrained at the nozzle ends. The boundary conditions of different models were distinguished from each other. Symmetries have been employed on different planes. In Fig. 2-a the end nozzle sections were constrained for the full pressure vessel model so that all the degrees of freedom are zero at the constrained ends. For the half pressure vessel in Fig. 2-b, there was a boundary condition of no axial movement at the transversal mid plane and the nozzle end shown has all DOF as zero. Similarly in Fig. 2-c to Fig. 2-f the nozzle side was constrained, no axial movement at the transversal plane and longitudinal midplane is employed and symmetric boundary conditions were used at the other segment of the pressure vessel, as shown in Fig. 2-g, so

that the computational time could effectively be reduced for static structural analysis. From reduced models we took advantage of the body and loading symmetry about the XY, YZ, and ZX planes by constraining the motions in the required directions

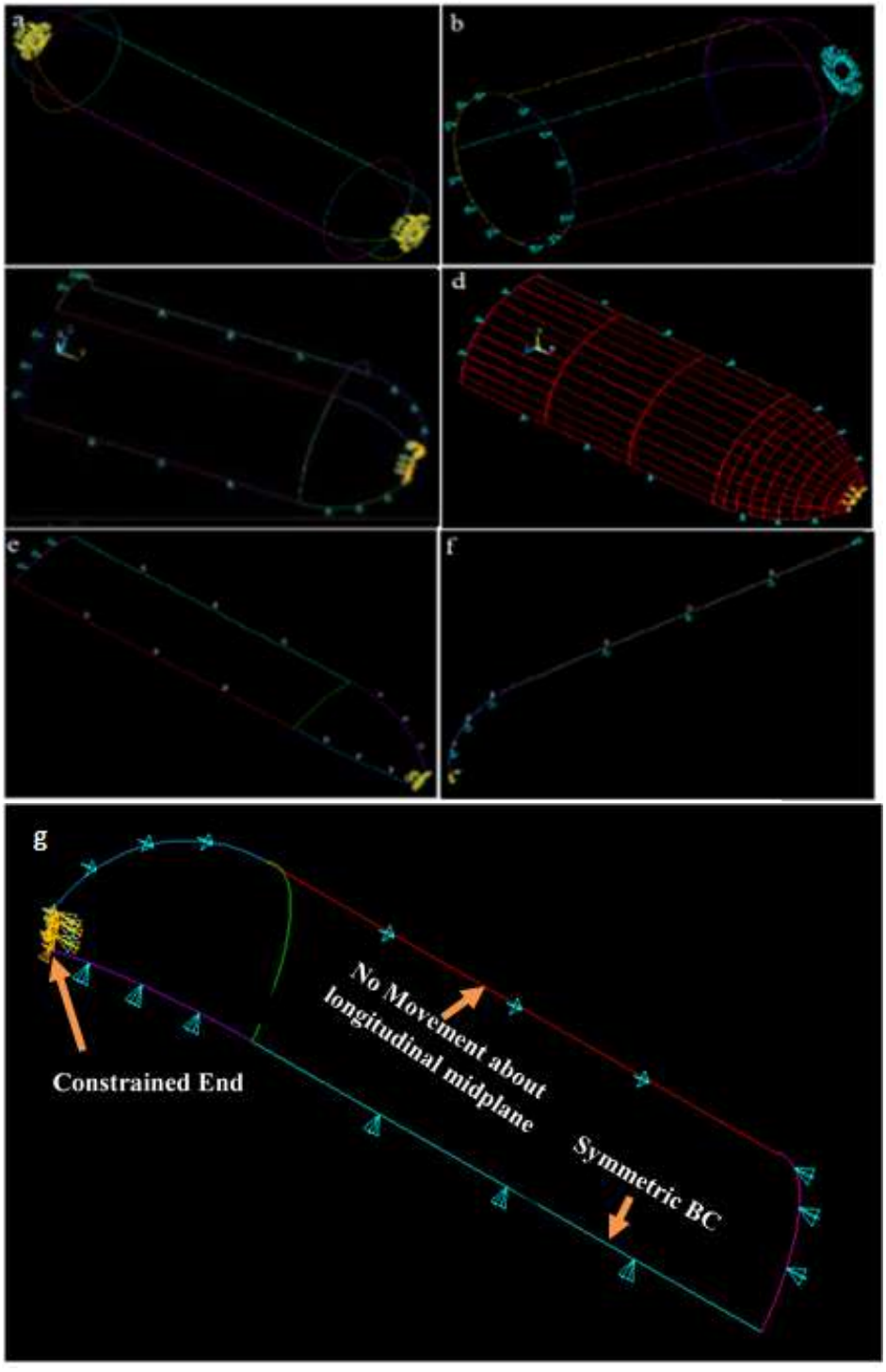

FIG. 2 (a-f) Boundary and Loading Conditions. (g) Boundary Conditions for 90^o Rotated Reduced Model

4.2 | Material Properties

Mechanical properties of composite materials used in simulation are listed in Table 2.

TABLE 2 Mechanical Properties of Graphite/Epoxy.

E_{11}	E_{22}	E_{33}	ν_{12}	ν_{13}	ν_{23}	G_{12}	G_{13}	G_{23}
128.5GPa	9.135GPa	9.135GPa	.249	.249	.249	5.7GPa	5.7GPa	3.66GPa

4.3 | Mesh Convergence Analysis

Reduced models were easy to mesh, and no. of elements and nodes reduced drastically from about 10,000 elements for the full model to 54 for the 1° model as shown in Fig. 10. These model results are less computationally intensive also static structural analysis time has been reduced effectively and efficiently. Failure was predicted using the 4x mentioned criteria.

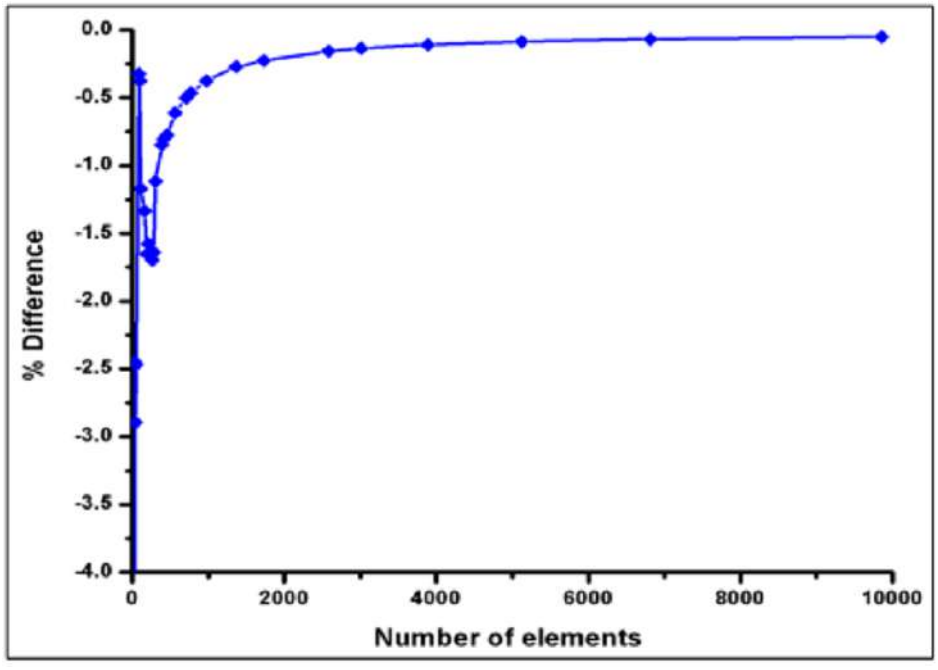

FIG. 3 Mesh convergence.

5 | RESULTS AND DISCUSSION

Layer 1 and layer 2 behavior under von mises stresses were investigated for the full model and reduced models. Stress distributions in different sections of the pressure vessel are shown below figures which is indicating maximum stresses and minimum stresses for layer 1 and layer 2. Maximum stresses for layer 1 occurred in the cylindrical section and for layer 2 maximum stresses occurred in the junction of the hemispherical and cylindrical region.

Full pressure vessel Von Mises stress distributions are shown in Fig. 4 for both layers. Layer 1 stresses were about 183 MPa and maximum in the hoop section of the pressure vessel. In layer 2 maximum stresses occurred in the junction of the hemispherical and the cylindrical region due to a sudden change in the winding angle of the composite layer transversally reinforced across the junction. Maximum stresses of about 121

MPa were induced. The values of results presented in Fig. 4 were very close to T.-H. L. Meng-Kao Yeh et al [11] results, hence benchmarking were satisfying.

| Full Pressure Vessel Von Mises Stresses

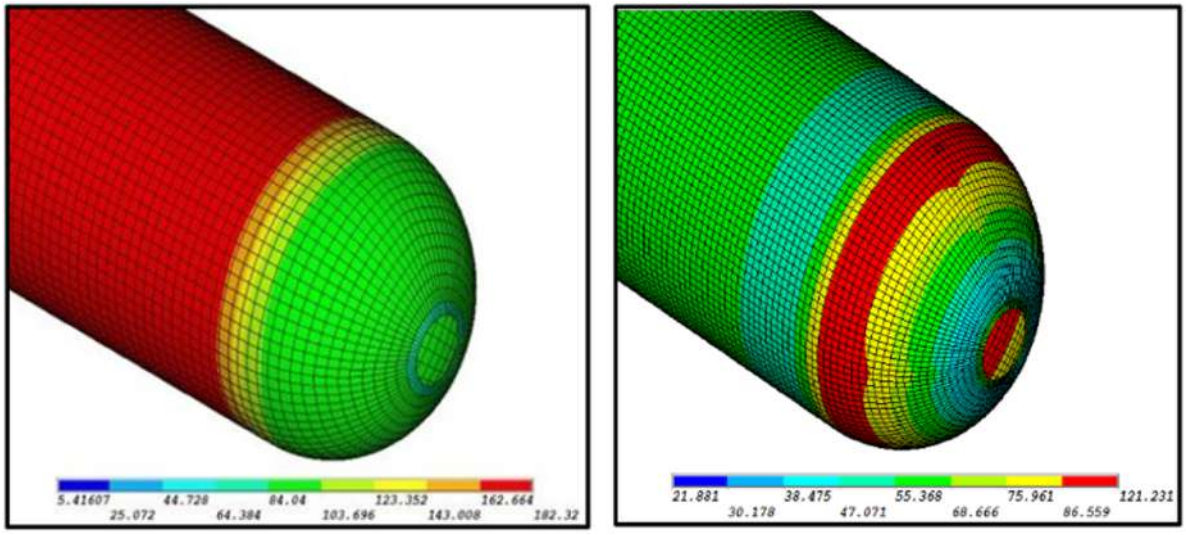

FIG. 4 Full Pressure Vessel Von Mises Stresses in (a) layer 1 (b) layer 2.

| Reduced Models Von Mises Stresses

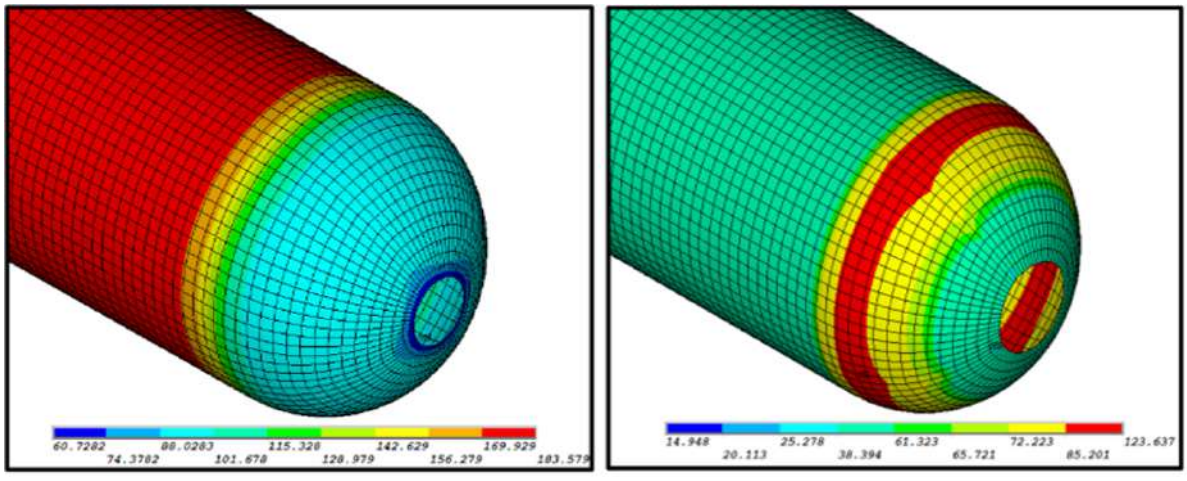

FIG. 5 Half Pressure Vessel Von Mises Stresses in (a) layer 1 (b) layer 2.

A comparison of different pressure vessel models was done under the same working conditions to reduce the size of the problem, hence computational power, cost, and time can effectively be reduced. Von Mises stresses in layer 1 of the half model are 183.6 MPa and 123.6 MPa for layer 2 as shown in Fig. 5. Results were well matched with the full model results, those were 183 MPa for layer 1 and 121 for layer 2. Hence, the model validity was confirmed and could be used for further studies. In Fig. 6, Von Mises stress results for element rotation at 90° are 183.8 MPa for layer 1 and 120MPa for layer 2. Results were very close to the full

model of the pressure vessel. Fig. 7 represented a model in which the element rotated at 45 °. The results of Von Mises stress for layer 1 is 184Mpa and for layer 2 it is 125.5MPa. It is indicated that values are too concise with full model results.

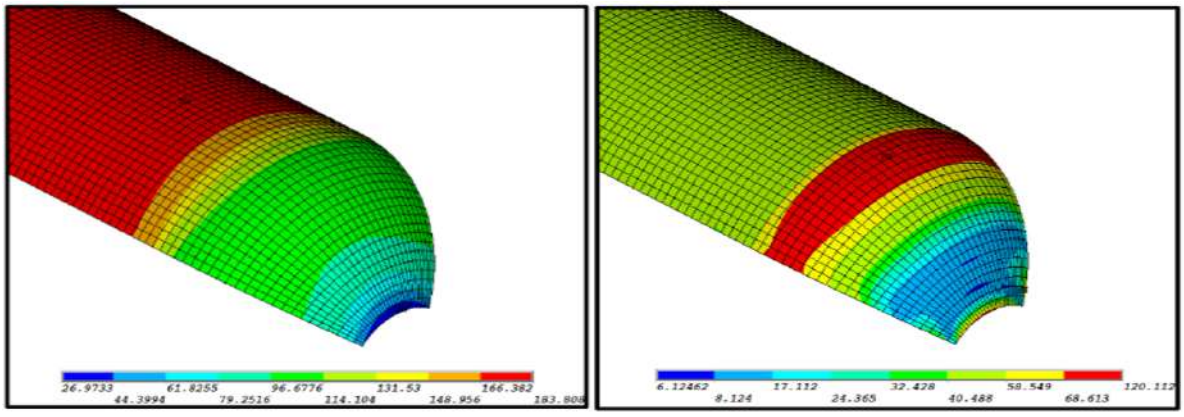

FIG. 6 Von Mises Stresses in 90° element rotation in (a) Layer 1 (b) Layer 2.

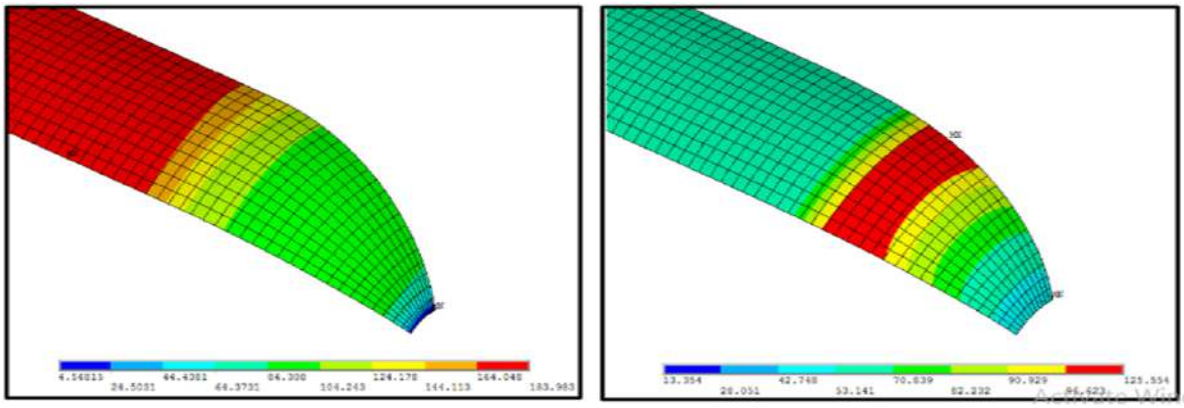

FIG. 7 Von Mises Stresses in 45° element rotation in (a) Layer 1 (b) Layer 2.

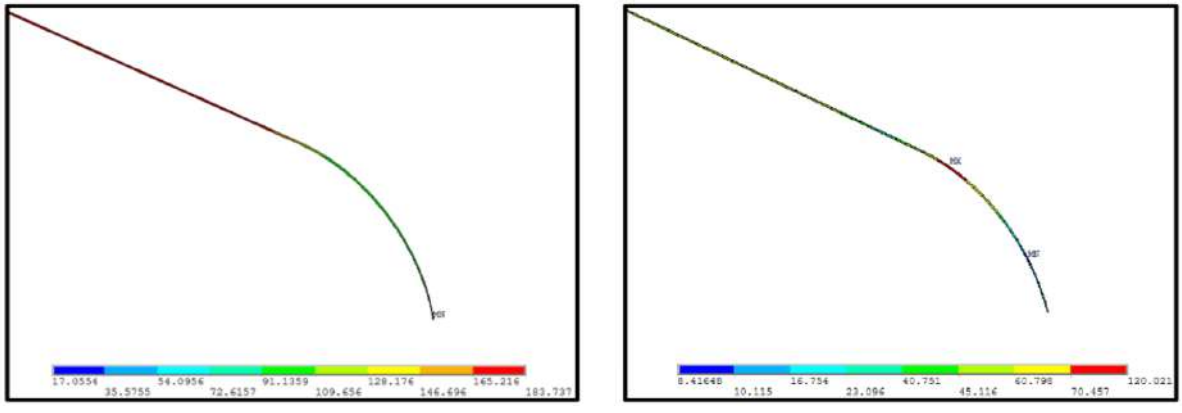

FIG. 8 Von Mises Stresses in 1° element rotation in (a) Layer 1 (b) Layer 2.

Fig. 8 shows that the Von Mises stresses are matched with the full model after comparing it with 1° rotation Von Mises results. Results are 183.7 MPa for layer 1 and 120 MPa for layer 2 which is fully satisfied with full model values. Similarly, Fig. 9 represented the results of von Mises for .1° rotated element in which 183 MPa for layer 1 and 119.8 MPa for layer 2 which is fully satisfied with full model values.

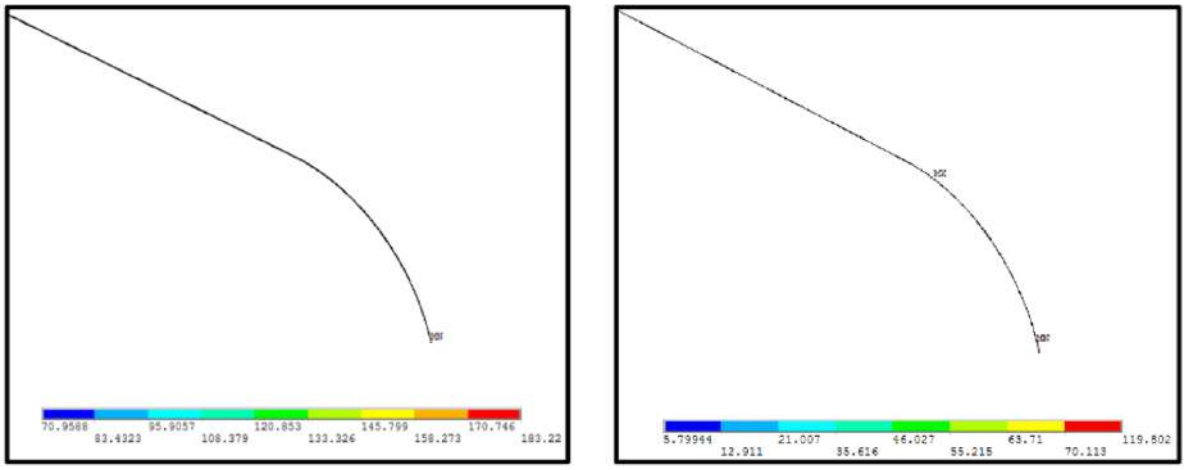

FIG. 9 Von Mises Stresses in .1° element rotation in (a) Layer 1 (b) Layer 2.

5.1 | Discussions related to failures

| Full Pressure vessel

Longitudinal stresses for layer 1 of the full pressure vessel were in the range of 166- 186 MPa in the cylindrical region and up to 60 MPa in the semispherical region. The tensile strength of the composite is around 1447MPa in the longitudinal direction and 51.7 MPa in the transverse direction.

TABLE 3 Comparison of Full Model and Reduced Model Failure criteria results.

	Layer 1				Layer 2			
Model	Tsai Wu	Tsai Hill	Smax	Von Mises (Safety Factor)	Tsai Wu	Tsai Hill	Smax	Von Mises (Safety Factor)
Full	0.556	0.554	0.081	7.9	3.208	2.27	1.73	0.427
Half	0.025	0.025	0.082	7.88	3.32	2.964	0.637	0.428
90	0.02	0.637	0.083	7.87	2.97	2.62	1.71	0.430
45	0.037	0.037	0.081	7.86	3.26	2.69	1.79	0.412
1	0.019	0.623	0.082	7.88	2.94	2.59	1.71	0.430
0.1	0.019	0.019	0.080	7.9	2.93	2.58	1.71	0.431

Stresses encountered in the transverse direction were in the range of 5-7 MPa in both cylindrical and semi-spherical regions for layer 1. As compared to generated stresses, the pressure vessel's layer 1 can withstand the stresses without failure. Longitudinal stresses for layer 2 were in the range of 70-124 MPa. Stresses in the direction perpendicular to the reinforcement directions declared the failure of layer 2. High stress was generated in the junction of cylindrical and semi-spherical dome due to the change in fiber direction from one region to another. No failure or deformation will be resulted in composite layer 1 under maximum longitudinal stress 186MPa due to the high strength of layer 1 around 1.45GPa as fibers were oriented longitudinally. However, composite layer 2 failed to sustain 124MPa because of the orientation of fiber in the transverse direction. The transverse strength of the composite was around 51.7MPa and layer 2 failure resulted because transverse strength was much lower than generated stresses. Maximum Stresses were generated in the longi-

tudinal direction, but no failure resulted due high strength of the composite, however, layer 2 deformed due to low transverse strength but due to the lining of layer 1 over layer 2 as shown in Fig. 1 no appreciable failure resulted because layer 1 sustained all the stresses and deformations.

According to Tsai Wu failure criteria, the value comes out to be less than 1 for the first layer but the second layer, the value was 3.208. It tells us the failure of layer 2 under Tsai Wu criteria. Tsai Hill criteria also predicted the same trend as for layer 1 the value was less than 1 but for layer 2 it was 2.27. Maximum stress criteria affirmed the results of Tsai Wu and Tsai Hill failure theory resulting in values of less than 1 for layer 1 and 1.73 for layer 2. All three failure criteria predicted the failure of layer 2 for the composite pressure vessel under the static structural analysis. The Von Mises stresses indicated the failure of layer 2 due to a safety factor of less than 1.

TABLE 4 Stress Distributions and Percent Error.

Model	Half	90	45	1	0.1
Stress (MPa)	183.579	183.808	183.983	183.737	183.22
% Error	0.867	0.993	1.089	0.954	0.670

| Reduced Models

Tsai Wu, Tsai Hill, and Maximum stress failure criteria applied on the Reduced models predicted the same results of safe working for composite layer 1 but the failure of layer 2 of the composite pressure vessel. The longitudinal stresses in Layer 1 of all Reduced models approached Full pressure vessel longitudinal stress, hence no failure occurred in layer 1. The failure resulted in layer 2 due to exceeding the stress limit. The utilization of Reduced models with their mentioned advantages in comparison to the full pressure vessel could be adapted to save time, cost, etc. Results of failure criteria in comparison with the full model are shown in Table 3.

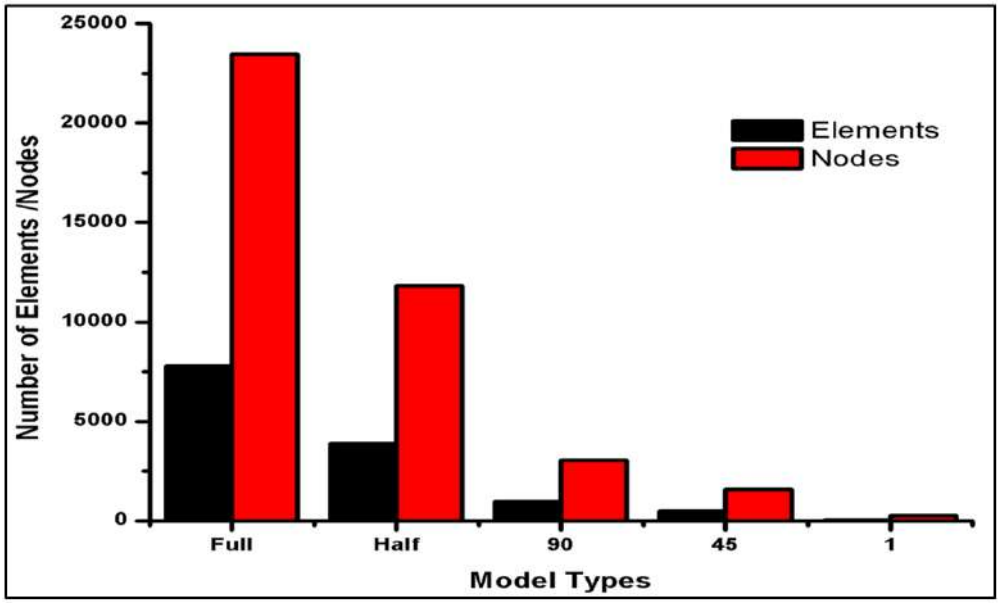

FIG. 10 Model Type vs No. of Elements and Nodes.

Von Mises stress distributions of the different reduced models are shown in Table 4. Half pressure vessel results are 183.579 MPa which has an error of 0.867 %. For 90°, 45°,1°, and 0.1° rotated sections of the pressure vessels the results are 183.808, 183.983, 183.737, and 183.22 respectively with the percentage

error of 0993, 1.089, 0.954, and 0.607 simultaneously. It is clear from the results that the difference between the results of different reduced models is very low, and the results are nearly the same as those of the full pressure vessel model. Reduced models can effectively supersede the full model. The reduction in the number of nodes and elements for reduced models is shown in Fig. 10. A comparative approach between no of nodes and elements of reduced model and full model revealed that reduced model 1° having 54 elements was almost 95% accurate with full model results of 7776 elements.

6 | CONCLUSIONS

No of nodes and elements for the full model is much greater than reduced models which increased the computing cost and time. Computational time and power were effectively reduced as indicated from the reduction of elements from 7776 for the full model to 54 for the 1° reduced model employed for the analysis. Von mises stress distributions for reduced models in comparison with full model indicated the accuracy of models and the 1° reduced model was 95% accurate having 273 nodes and 54 elements. Reduced models predicted accurate results and can supersede the full model efficiently. A comparative study of the failure criterion's results between reduced models and full models predicted the failure of layer 2. All failure criteria resulted in the failure of layer 2 of the vessel in the transition region, therefore any of the failure criteria can be employed to access the model behavior.

Declaration of Interest

The authors declare that there is no conflict of interest.

References

[1] M. Azeem and H. H. Ya, "Application of filament winding technology in composite pressure vessels and challenges," *A Review" Journal of Energy Storage*, vol. 49, 2022-05. **DOI:** 10.1016/j.est.2021.103468

[2] E. N. a, "Experimental and numerical analysis of a lldpe/hdpe liner for a composite pressure vessel," *Polymer Testing*, p. 693–700, 2011. **DOI:** 10.1016/j.polymertesting.2011.04.016

[3] J. P.Xu, "Finite element analysis of burst pressure of composite hydrogen storage vessels," *Materials and design*, p. 2295–2301, 2009. **DOI:** 10.1016/j.matdes.2009.03.006

[4] A. S. Chauhan, "Design and analysis of high pressure composite vessels," *International Journal of Latest Engineering and Management Research (IJLEMR*, p. 96–102, 2018-06. [Online] Available: http://www.ijlemr.com/papers/volume3-issue6/16-IJLEMR-33237.pdf.

[5] S. A. S and S. S. Bhat, "et.al ,"finite element analysis of composite overwrapped pressure vessel for hydrogen storage," in *2016 Intl. Conference on Advances in Computing, Communications and Informatics (ICACCI*, (Jaipur, India, Sept), p. 21–24, 2016. **DOI:** 10.1109/icacci.2016.7732083

[6] K.-S. Park, "Analysis of filament wound composite structures considering change of winding angles through the thickness direction," *Composite Structures*, vol. 55, p. 63–71, 2002.

[7] V. Vasiliev, A. Krikanov, and A. Razin, "New generation of filament-wound composite pressure vessels for commercial applications," *Composite structures*, vol. 62, no. 3-4, pp. 449–459, 2003. **DOI:** 10.1016/s0263-8223(01)00137-4

[8] M. Kabir, "Finite element analysis of composite pressure vessel with load sharing metalic liner," *Composite Structures*, vol. 49. **DOI:** 10.1016/s0263-8223(99)00044-6

[9] M. Dimitrijević and N. et.al, "Modeling of the mechanical behavior of fiber-reinforced ceramic composites using finite element method (fem," *Science of Sintering*, p. 385–390, 2014. **DOI:** 10.2298/sos1403385d

[10] Z. Yue, "Xiaohui li "numerical simulation of all-composite compressed natural gas (cng) cylinders for vehicle." **DOI:** 10.1016/j.proeng.2012.04.197

[11] T.-H.-K. Yeh, "Finite element analysis of graphite/epoxy composite pressure vessel," *Journal of Materials Science and Chemical Engineering*, pp. 5, 19–28, 2017. **DOI:** 10.4236/msce.2017.57003

[12] B. E. Reddy, "Axis symmetric stress analysis of internally pressurized rotating cylinder with different materials by using ansys," *Anveshana's International Journal of Research In Engineering and Applied Sciences*, vol. 2, no. Issue 3, 2017-03.

[13] Y. Shao, "Andrea betti et.al "high pressure strength of carbon fibre reinforced vinylester and epoxy vessels," *Composite Structures*, 2015-12. **DOI:** 10.1016/j.compstruct.2015.12.053

[14] I. Demir, "Oner saymen et.al "the effects of repeated transverse impact load on the burst pressure of composite pressure vessel," *Composite Part B : Engineering*, vol. 68, 2015-01. **DOI:** 10.1016/j.compositesb.2014.08.038

[15] JCVelosa, "Development of a new generation of filament wound composite pressure cylinders," *Composites Science and Technology*, vol. 69, p. 1348–1353, 2009. **DOI:** 10.1016/j.compscitech.2008.09.018

[16] R. Rafiee, "Theoretical study of failure in composite pressure vessels subjected to low-velocity impact and internal pressure," *Frontiers of Structural and Civil Engineering*, vol. 14, p. 1349–1358, 2020. **DOI:** 10.1007/s11709-020-0650-3

[17] R. Chang, "Experimental and theoretical analyses of first-ply failure of laminated composite pressure vessels"," *Compos. Struct*, vol. 49, no. 2, p. 237–243, 2000. **DOI:** 10.1016/s0263-8223(99)00133-6